HHS Public Access

Author manuscript

J Immunol. Author manuscript; available in PMC 2016 August 01.

Published in final edited form as:

J Immunol. 2015 August 1; 195(3): 924–933. doi:10.4049/jimmunol.1500070.

A novel glycolipid antigen for NKT cells that preferentially induces IFN-γ production

Alysia M. Birkholz[*,†,‡], **Enrico Girardi**[†], **Gerhard Wingender**[*], **Archana Khurana**[*], **Jing Wang**[†], **Meng Zhao**[*], **Sonja Zahner**[*], **Petr A. Illarionov**[§], **Xiangshu Wen**[¶], **Michelle Li**[¶], **Weiming Yuan**[¶], **Steven A. Porcelli**[‖], **Gurdyal S. Besra**[§], **Dirk M. Zajonc**[†], and **Mitchell Kronenberg**[*,‡]

[*]Division of Developmental Immunology, La Jolla Institute for Allergy & Immunology, La Jolla, CA 92037, USA

[†]Division of Cell Biology, La Jolla Institute for Allergy & Immunology, La Jolla, California 92037, USA

[‡]Division of Biological Sciences, University of California, San Diego, La Jolla, California 92037, USA

[§]School of Biosciences, University of Birmingham, Edgbaston, Birmingham B15 2TT, UK

[¶]Department of Molecular Microbiology and Immunology, Keck School of Medicine, University of Southern California, Los Angeles, CA 90033, USA

[‖]Department of Microbiology and Immunology, and Department of Medicine, Albert Einstein College of Medicine, Bronx, New York 10461, USA

Abstract

Here we characterize a novel Ag for invariant natural killer T-cells (*i*NKT cells) capable of producing an especially robust Th1 response. This glycosphingolipid (GSL), DB06-1, is similar in chemical structure to the well-studied α-galactosylceramide (αGalCer), the only change being in a single atom, the substitution of a carbonyl oxygen with a sulfur atom. Although DB06-1 is not a more effective Ag *in vitro*, the small chemical change has a marked impact on the ability of this lipid Ag to stimulate *i*NKT cells *in vivo*, with increased IFN-γ production at 24 h compared to αGalCer, increased IL-12, and increased activation of NK cells to produce IFN-γ. These changes are correlated with an enhanced ability of DB06-1 to load in the CD1d molecules expressed by DCs *in vivo*. Moreover, structural studies suggest a tighter fit into the CD1d binding groove by DB061 compared to αGalCer. Surprisingly, when *i*NKT cells previously exposed to DB06-1 are restimulated weeks later, they have greatly increased IL-10 production. Our data are therefore consistent with a model whereby augmented and or prolonged presentation of a glycolipid Ag leads to increased activation of NK cells and a Th1-skewed immune response, which may result in part from enhanced loading into CD1d. Furthermore, our data suggest that strong antigenic

Corresponding author: Mitchell Kronenberg, Phone: 858.752.6500, Fax: 858 752 6990, Mitch@liai.org.

[1]Current address of Enrico Girardi: CeMM, Research Center for Molecular Medicine of the Austrian Academy of Sciences, A-1090 Vienna, Austria

stimulation *in vivo* may lead to the expansion of IL-10 producing *i*NKT cells, which could counteract the benefits of increased, early IFN-γ production.

Introduction

Type 1 or invariant NKT (*i*NKT) cells are a lymphocyte population that is characterized by features of both the innate and adaptive immune responses. The multiple functions of these cells are remarkable in that they have been implicated in allergy, cancer, infection, autoimmunity, and a variety of other conditions (1). Similar to other T lymphocytes, *i*NKT cells arise from a $CD4^+$, $CD8^+$ double positive thymocyte precursor (2). Unlike mainstream, T cells, which recognize peptide moieties presented by major histocompatibility complex (MHC)-encoded molecules, *i*NKT cells recognize lipid Ags that are often glycosphingolipids (GSLs). Lipid Ags are recognized when they are presented by CD1d, a MHC class-I-like molecule (3). The CD1d binding groove is composed of two hydrophobic pockets labeled A′ and F′(4). GSLs bind with the fatty acid localizing into the A′ groove and the sphingoid base into the F′ groove. This binding mode allows the carbohydrate headgroup to protrude out of the CD1d molecule such that it is exposed to be recognized by the *i*NKT cell TCR (5).

The *i*NKT cell TCR contains a highly restricted, invariant TCR α chain that is formed by a Vα14-Jα18 rearrangement in mice, and a homologous Vα24-Jα18 (TRAV10- TRAJ18) in humans (6). Although the β chain of these TCRs is not invariant, it is biased to Vβ8.2, Vβ7 or Vβ2 in mice, and Vβ11 (TRBV25-1) in humans, with diverse CDR3 regions.

The prototypical GSL recognized by *i*NKT cells is alpha galactosylceramide (αGalCer) (7, 8). When stimulated by a strong agonist, such as αGalCer, *i*NKT cells secrete both Th1 and Th2 cytokines, such as IFN-γ and IL-4 (9). Stimulation with αGalCer causes long-term changes in the *i*NKT cell population that have been originally likened to anergy (10, 11). We recently showed that stimulation with αGalCer leads to an expansion of an *i*NKT cell population capable of secreting IL-10, referred to as NKT10 cells (12). Interestingly, subtle chemical/structural alterations in αGalCer have been shown to alter the down-stream cytokine response, skewing it towards either a Th1 or a Th2 phenotype (13). Generation of an Ag capable of stimulating a strong Th1 cytokine profile has been an area of great interest, because this would be beneficial for stimulating for anti-cancer responses and for use as a vaccine adjuvant. Based on prior work, a heightened IFN-γ response is due, in large part, to the so-called *trans*-activation of NK cells occurring downstream of *i*NKT cell stimulation (14–16). Therefore, a strong Th1 response induced by this and some other GSL Ags represents not so much the tendency of an *i*NKT cell to produce more IFN-γ with reduced IL-4, but represents the output of a cellular network that involves dendritic cells (DCs) expressing CD1d, *i*NKT cells to activate the response, and NK cells that are stimulated downstream of *i*NKT cells that are crucial for continued IFN-γ release.

Although αGalCer has been shown to suppress tumor metastases in mouse models (8), it has not been overwhelmingly successful in human trials, possibly due in part to the mixed Th1 and Th2 response or the anergy it induces (17, 18) or due to the potential induction of NKT10 (12). Because of this, many analogs of αGalCer have been generated in attempts to

elicit a more pronounced Th1 skewed response. C-glycoside, which differs from αGalCer by replacing the carbon-oxygen glycosidic linkage with a carbon-carbon bond, was the first GSL Ag reported to have a Th1 polarizing potential (19, 20). C-glycoside cannot stimulate human *i*NKT cells and can therefore is not useful for therapeutic applications.

Here we characterized in detail the biochemical properties, immune responses and mechanisms of action of a novel αGalCer analog, DB06-1. This compound is identical to αGalCer except for the replacement of the C2 carbonyl oxygen on the acyl chain with a sulfur atom. DB06-1 was identified in a screen of lipids that associated with detergent resistant membrane domains, which is characteristic for other Th1 skewing Ags tested to date (21). Here we provide evidence that DB06-1 promoted a Th1 skewed response that was more prominent than αGalCer. This was correlated with increased loading of this antigen into CD1d, which may be related to a tighter fit in the CD1d groove. However, over the longer term, DB06-1 induced more IL-10 producing NKT10 cells than αGalCer, suggesting that the Th1 effect of a strong antigenic stimulus may induce a counter regulatory pathway *in vivo*.

Materials and Methods

Statistical tests

Unless otherwise noted, statistical comparisons were drawn with a 2-tailed Student T-tests were used. The symbols used in the figures are as follows: ns $P > 0.05$, * $P \leq 0.05$, ** $P \leq 0.01$, *** $P \leq 0.001$, **** $P \leq 0.0001$

Cell-free antigen presentation assay

Stimulation of *i*NKT cell hybridomas on microwell plates coated with soluble mouse CD1d was carried out according to published protocols (23–25). The indicated amounts of compounds or vehicle were incubated for 24 h in microwells that had been coated with 1.0 μg of CD1d. After washing, 5×10^4 DN3A4-1.2 (called 1.2 here) Vα14 *i*NKT hybridoma cells were cultured in the plate for 24 h, and IL-2 in the supernatant was measured by sandwich ELISA (R&D Systems) following the manufacturer's instructions. The 1.2 Vα14 *i*NKT cell hybridoma expresses a Vα14-Vβ8.2 TCR and has been described previously (26).

Antigen presentatoin assays

The culture of bone-marrow derived DC in GM-CSF has been described previously (27). Briefly, cells were isolated from mouse femurs and were cultured in media containing GM-CSF for 7 days. The cells were then pulsed with GSL Ags overnight and were incubated with 5×10^4 1.2 Vα14 *i*NKT hybridoma cells for 20–24 h. Similarly, the antigen presentation assay using A20 B lymphoma cells has been described (28). Briefly, A20-CD1d transfectants expressing wild type (WT) CD1d or tail deleted (TD) CD1d were pulsed with a GSL Ag overnight. APCs (1×10^5 per well) were incubated with 5×10^4 *i*NKT hybridomas for 20–24 h. IL-2 in the supernatant of hybridoma cultures was measured by sandwich ELISA (R&D Systems). Human $V\alpha24^+$ *i*NKT cells were purified by magnetic enrichment and expanded according to a previously published protocol (29). Briefly, PMBCs were isolated by Percoll (Sigma) density-gradient centrifugation. Human donor PBMCs (1–

1.5×10^6/ml) were cultured in RPMI 1640 (Invitrogen) supplemented with 10% (v/v) FBS and 1% (v/v) Pen-Strep-Glutamine (10,000 U/ml penicillin, 10,000 g/ml streptomycin, 29.2 mg/ml L-glutamine; Invitrogen). Human *i*NKT cell cultures were expanded by weekly re-stimulation with αGalCer-pulsed, irradiated PBMCs and recombinant human IL-2. Ag-pulsed PBMCs (1×10^5/well) were seeded in 96 well plates and cultured in the presence of 5×10^4 Vα24$^+$ human *i*NKT cells for 20–24 h. GM-CSF release, as a marker of *i*NKT cell activation, was measured by sandwich ELISA (R&D Systems).

Mice

C57BL/6 mice were purchased from The Jackson Laboratory. CD1-TD mice were generously provided by the laboratory of Dr. Albert Bendelac (30). *Cd1d*$^{f/f}$ mice were generated in the laboratory using conventional strategies and were crossed with a *CD11c-Cre* transgenic mice obtained from The Jackson Laboratory (31). IL-12$^{-/-}$ (strain B6.129S1-*Il12a*^{tm1Jm}/J) mice were also purchased from The Jackson Laboratory. All mice were housed in specific pathogen-free conditions and the experiments were approved by the Institutional Animal Care and Use Committee of the La Jolla Institute for Allergy & Immunology. Humanized mice (hCD1d-Vα24 Tg) (Wen et al., submitted) were generated by crossing a human CD1d knockin mouse line (32) and a human Vα24 TCR mouse line (33) and tested in the lab of Weiming Yuan following Animal Care and Use guidelines of the University of Southern California. Mice were injected with 1–4 μg of DB06-1 or αGalCer intravenously, αGalCer provided a positive control and blood serum or spleens were harvested either at 2, 6, 22, or 24 h later or in the case of NKT10 staining, 4 weeks later. Standard sandwich ELISAs for mouse IFN-γ, IL-12p70, and IL-4 (R&D Systems) were performed to measure cytokines in the sera.

Cell preparation

Single cell suspensions of splenocytes were generated as described previously (34). For DCs isolation, the tissue was diced into 1mm pieces, digested using spleen dissociation media (Stem Cell Technologies) and DCs were enriched by positive selection using a CD11c$^+$ isolation kit (Stem Cell Technologies) or MACS Technology according to the manufacturer's protocols (Miltenyi Biotec). Isolated DCs were co-cultured at varying concentrations with 5×10^4 1.2 Vα14 *i*NKT hybridoma cells overnight and activation was measured by sandwich ELISA of culture supernatants for IL-2.

Flow cytometry and intracellular cytokine staining

For IFN-γ ICCS staining, the cells were cultured in media consisting of RPMI 1640 (Invitrogen) supplemented with 10% (v/v) FBS and 1% (v/v) Pen-Strep-Glutamine (10,000 U/ml penicillin, 10,000 g/ml streptomycin, 29.2 mg/ml L-glutamine; Invitrogen) for 4 h at 37°C in the presence of GolgiPlug (BD Biosciences). To measure NKT10 cell IL-10, splenocytes were isolated from mice and were re-stimulated with PMA (0.1 μg/mL) and ionomycin (0.9 μg/mL) (both from Sigma-Aldrich) for 4 h at 37°C in the presence of GolgiPlug and GolgiStop in media consisting of RPMI 1640 (Invitrogen) supplemented with 10% (v/v) FBS and 1% (v/v) Pen-Strep-Glutamine (10,000 U/ml penicillin, 10,000 g/ml streptomycin, 29.2 mg/ml L-glutamine; Invitrogen). Single-cell lymphocyte suspensions

were purified by use of Lymphoprep (Axis-Shield, Oslo, Norway) density gradient centrifugation. Anti-mouse CD16/32 antibody (2.4 G2), isolated in our laboratory, was used for Fc receptor blocking. Antibodies used in experiments were, CD1d-αGalCer tetramers labeled with the fluorochrome BV421 (BD Biosciences) (generated in our laboratory) (35), CD45R/B220 (BD Biosciences), NK1.1 (eBiosciences), CD8 (BD Biosciences), CD4 (Life Technologies), TCRβ (BioLegend), CD3ε (BioLegend), CD44 (BD Biosciences), CD19 (BioLegend), IFN-γ (eBiosciences), IL-10 (BD Biosciences), CD11c (eBiosciences), CD11b (BD Biosciences), CD40 (BD Biosciences), CD86 (BD Biosciences), CD80 (BD Biosciences), CD1d (BD Biosciences), and L363 (BioLegend). Dead cells were labeled with Live/dead yellow or aqua (Life Technologies). The cells were then fixed and permeabilized using Cytofix/Cytoperm buffer (BD Biosciences). The data were collected on a LSR II or Fortessa flow cytometers (BD Biosciences) and analyzed using FlowJo software (Tree Star).

NK cell depletion

C57BL/6 mice were depleted of NK cells by injecting 50 μl anti-asialo GM1 rabbit polyclonal Ab (Wako) 24 h prior to Ag challenge. NK cell depletion ($NK1.1^+$ $TCR\beta^-$ cells) was verified by flow cytometry.

Mouse CD1d expression, purification and TCR refolding

Mouse CD1d-β2-microglobulin heterodimeric protein was expressed in a baculovirus expression system as reported previously (36). Human CD1d-β2-microglobulin was prepared similarily to the mouse protein. The Vα14-Vβ8.2 TCR construct design, refolding and purification processes were identical to the ones previously reported (37), while the autoreactive human Vα24-Vβ11 TCR (auto-Vα24) 4C1369 (38, 39) was generously provided by Dr. Jamie Rossjohn and prepared as reported (40).

Glycolipid loading and DB06-1-CD1d-TCR complex formation

The DB06-1 lipid synthesized in the laboratory of Gurdyal S. Besra, was dissolved in DMSO at 1mg/ml. Before loading, 25 μl was diluted to 0.25 mg/ml with 25 μl vehicle solution (50 mM Tris-HCl pH 7.0, 4.8 mg/ml sucrose, 0.5 mg/ml sodium deoxycholate and 0.022% Tween 20) and 50 μl 1% Tween 20 and incubated at 80°C for 20 min. DB06-1 was loaded onto CD1d overnight (molar ratio of protein to lipid of 1:3) in the presence of 10 mM Tris-HCl pH 7.0. Refolded TCR was incubated at room temperature for 1 h with lipid-loaded CD1d at a 1:2 molar ratio and the ternary CD1d-lipid-TCR complex was isolated from uncomplexed CD1d and TCR by size exclusion chromatography using Superdex S200 10/300 GL (GE Healthcare).

Surface plasmon resonance binding analysis

Surface plasmon resonance (SPR) binding studies were conducted using a Biacore 3000 as reported previously (37). Briefly, approximately 300 response units of biotinylated CD1d (either human or mouse) loaded with DB06-1 were immobilized onto a streptavidin sensor chip (GE Healthcare) surface by injecting the CD1d-DB06-1 mixture at 3 μl/min in Hepes buffered saline (HBS) running buffer. A reference surface was generated in another flow channel with unloaded CD1d. Mouse or autoreactive human TCR were flowed over at a

constant rate. Experiments were carried out at 25°C with a flow rate of 30 μl/min and were performed at least twice. Kinetic parameters for the mouse molecule interactions were calculated after subtracting the response to CD1d molecules in the reference channel, using a simple Langmuir 1:1 model in the BIAevaluation software version 4.1. Human kinetic parameters were obtained using steady state solution graphs plotting T_{eq} vs concentration and were fitted with binding response at equilibrium using BIAevaluation software version 4.1.

Crystallization and structure determination

The mouse CD1d-DB06-1-TCR complex was isolated by Superdex S200 10/300 GL (GE Healthcare) column chromatography in 50 mM Hepes pH 7.4, 150 mM NaCl and concentrated to 0.86 mg/mL. Crystals were grown at 22.3°C by sitting drop vapor diffusion while mixing 2 μl protein with 2 μl precipitate (0.2M ammonium citrate dibasic pH 4.98 20% PEG 4000). Crystals were then flash-cooled at 100°K in mother liquor containing 20% glycerol. Diffraction data were collected at the Stanford Synchrotron Radiation Laboratory beamline 11-1 and processed with the software Mosflm (41). The CD1d-DB06-1-TCR crystallized in space group $C222_1$. The structure was solved by molecular replacement in CCP4 (Collaborative Computational Project, Number 4) (1994) using the protein coordinates from the CD1d-iGb3 structure as the search model [PDB code 2Q7Y] (42) as the search model followed by the *i*NKT cell TCR [PDB code 3QUZ] (43). The model was rebuilt into σA-weighted 2*Fo – Fc* and *Fo – Fc* difference electron density maps using the program COOT (44). The lipid was built into 2*Fo –Fc* map and refined using REFMAC (1994). The final refinement steps were performed using the TLS procedure in REFMAC with five domains (α1-α2 domain including carbohydrates and glycolipid, α3-domain, β2m, variable domain and constant domain of TCR). The CD1d-DB06-1-TCR structure was refined to 2.83 Å to an Rcryst and Rfree of 20.9% and 25.6% respectively. The quality of the model was excellent as assessed with the program Molprobity (45) (Supplemental Table I).

Results

DB06-1 activates mouse and human iNKT cells

DB06-1 is identical to αGalCer, with the exception of the replacement of the C2 carbonyl oxygen on the acyl chain for a sulfur atom (Fig. 1A). We used several assays to measure the antigenic potency of this compound. Initially, we tested DB06-1 in a cell-free antigen presentation assay, whereby a soluble CD1d molecule was coated on a plate, GSL Ags were added, and then IL-2 release from an *i*NKT cell hybridoma was used to determine if the lipid could activate the *i*NKT cell TCR. DB06-1 only weakly stimulated the *i*NKT cell hybridoma compared to αGalCer (Fig. 1B). We also used a cell-based antigen presentation assay, with bone marrow derived DCs as the APC. This a more physiologically relevant experimental setup as it allows for the uptake by APCs and endolysosomal loading of GSL Ags into CD1d. In this experimental set-up, DB06-1 was a more effective Ag, although it remained weaker in comparison to αGalCer (Fig. 1C).

As noted in the Introduction, some lipids that activate mouse *i*NKT cells do not stimulate their human counterparts, and therefore such compounds in this category are not relevant for the development of immune therapies. In order to address the possible utility of DB06-1, we preformed two studies. In the first, we determined if DB06-1could efficiently activate human *i*NKT cells derived from human blood. We showed that DB06-1 activated *i*NKT cells from two different donors using human PBMCs as CD1d expressing APCs (Fig. 2A). We also used a mouse strain in which the mouse *Cd1d1* gene was replaced with its human CD1d counterpart. These mice also contained a human *i*NKT cell Vα24 TCRα transgene and were crossed onto the $C\alpha^{-/-}$ background. We refer to this strain as *i*NKT cell humanized mice. To assess their immune response, we injected DB06-1 into these humanized mice and measured IFN-γ at 12 and 26 h post injection (Fig. 2B) and IL-4 at 2 h post injection (Fig. 2C). We note that IFN-γ in the sera of humanized mice was higher when mice were injected with DB06-1 as compared to αGalCer, whereas at the 2 h timepoint, IL-4 was decreased in the mice injected with DB06-1. In summary, these two studies indicate that DB06-1 is able to activate human *i*NKT cells and generate a Th1 response in a humanized *i*NKT cell mouse model.

DB06-1 promotes increased IFN-γ secretion

Th1 cytokine skewing following GSL stimulation is believed to be the product of a cellular network that responds within the first 24 h (16). We therefore analyzed the *in vivo* response to DB06-1 by measuring the concentration of cytokines (IFN-γ and IL-4) in the sera of mice 2 and 22 h after injection (Fig. 3A). Previous results (21), showed that DB06-1 can induce a robust serum IFN-γ *in vivo.* The initial IFN-γ response induced by DB06-1, measured at 2 h, was similar to the response induced by αGalCer (Fig. 3A and Supplemental Fig. 1A) and is due to the rapid IFN-γ secretion from *i*NKT cells. Although ICCS IFN-γ at 2 h was higher in mice injected with αGalCer compared to DB06-1, (Supplemental Fig. 1C and Supplemental Fig. 1D), this was not reflected in the sera data. The production of IFN-γ at 22–24 h after GSL injection has been attributed to the *trans*-activation of NK cells, due in part to IL-12 production from APCs (46–49). Serum IL-12 levels from mice injected with DB06-1 at 6 h post injection was higher than in mice injected with αGalCer (Fig. 3B). To measure NK cell *trans*-activation, we analyzed IFN-γ production of splenic NK cells from mice injected with DB06-1 24 h previously. After a 4 h culture with GolgiPlug, splenic NK cells ($NK1.1^{+}$ $TCR\beta^{-}$) were identified by flow cytometry and intracellular IFN-γ was measured. NK cells of mice injected with DB06-1 produced more IFN-γ than NK cells from αGalCer injected mice (Fig. 3C) with 11–24% of NK cells from mice injected with DB06-1 producing IFN-γ as compared to 1.5–6.5% of NK cells from mice injected with αGalCer (Supplemental Fig. 2A and Supplemental Fig. 2B). To further determine that the sera IFN-γ production at this 24 h time point was indeed due to NK cell *trans*-activation, we repeated the experiment in mice depleted specifically of NK cells using anti-asialo-GM1 antibodies (50) This treatment effectively depleted NK cells (Supplemental Fig. 2C and Supplemental 2D), but did not affect *i*NKT cells (Supplemental Fig. 2E). The serum IFN-γ levels at 24 h after DB06-1 injection were significantly lower in these NK cell depleted mice than in control mice (Fig. 3D). We also injected $Il12^{-/-}$ mice and measured serum IFN-γ at 24 h by ELISA. In the absence of IL-12, the amount of IFN-γ in the serum from mice injected with DB06-1 was reduced approximately 10-fold (Supplemental Fig. 2F). Intracellular cytokine staining

(ICCS) demonstrated that NK cells from DB06-1 injected *Il12*$^{-/-}$ mice did not produce IFN-γ (Supplemental Fig. 2G). Based on these data, we conclude that DB06-1 causes a strongly Th1 skewed response *in vivo*, in both *i*NKT cell humanized and WT mice. Furthermore, it acts by causing increased IL-12, which stimulates NK cells to produce IFN-γ, with NK cells providing the majority of IFN-γ in the serum.

DB06-1 is presented more effectively by DCs

A previous study has indicated that CD8α$^+$ CD11c$^+$ DCs are the dominant antigen presenting cell type essential for activation of *i*NKT cells by injected GSL Ags (51), although in some circumstances, macrophages have been shown to be important too, especially for Ags that are in particulate form (52). To determine if DCs were essential for the presentation of DB06-1, we generated a mouse strain with floxed CD1d alleles (*Cd1d*$^{f/f}$ *mice*) and crossed this line with a *CD11c-Cre* transgenic mouse strain (Cd1d$^{f/f}$ Cre$^+$ mice), thereby deleting CD1d expression on CD11c$^+$ cells, including most DCs (Fig. 4A). When Cd1d$^{f/f}$ Cre$^+$ mice were injected with DB06-1, we observed a significant decrease in the amount of IFN-γ in mouse sera at 24 h (Fig. 4B). However, as IFN-γ production was not completely absent, these data suggest that CD11c$^+$ DCs may not be the sole population capable of presenting DB06-1 to *i*NKT cells *in vivo*. IL-4 in the sera at 2 h was also determined and was decreased in Cd1d$^{f/f}$ Cre$^+$ mice as well (Supplemental Fig. 3A). Therefore, we conclude that CD11c$^+$ DCs likely were important for DB06-1 presentation *in vivo*, although the participation of other cell types was not excluded. To further investigate how αGalCer and DB06-1 might affect DCs, we analyzed surface markers on CD8α$^+$ DCs, comparing the 2 and 24 h time points. Surface levels of CD1d did not change in mice injected with either GSL Ag, however, CD80 and CD86 were increased at 24 h post injection of either αGalCer or DB06-1. There was a trend to higher expression of both CD80 and CD86 with injection of DB06-1 at 24 h but the difference was not significiant (Supplemental Fig. 3B)

We previously found that a common feature of several Th1 cytokine skewing αGalCer analogs is that they persist longer as complexes with CD1d on the surface of APCs *in vivo* (53). To address this, injected lipid Ags and we used an antibody that binds specifically to αGalCer-CD1d complexes (L363) to measure surface GSL-CD1d complexes on DCs using flow cytometry. After injection of either αGalCer or DB06-1, complexes with CD1d were barely detectable on the surface of DCs by flow cytometry at 2 h post injection, compared to control, uninjected mice. At 24 h, however, DB06-1-CD1d complex staining was higher and increased compared to the αGalCer-CD1d complex (Supplemental Fig. 3C).

We analyzed the presence of these complexes using a T cell functional assay, which is more sensitive than flow cytometry, as it is likely that very Ag-CD1d complexes are required to activate an *i*NKT cell. We injected mice with one of the GSL Ags, isolated a splenic fraction enriched for DCs at 2 h or 24 h, and used these APCs cells to stimulate *i*NKT cell hybridomas *in vitro* (13, 53). The Th1 skewing lipids that had been analyzed in this way previously showed an increased ability to activate *i*NKT cell hybridomas at 24 h compared to αGalCer (53). In accordance with these studies, we observed that APCs purified 24 h after Ag injection were indeed better able to activate *i*NKT cell hybridomas *in vitro* when

they had been exposed *in vivo* to DB06-1 than αGalCer (Fig. 4D). Unlike the previous studies, however, even at 2 h after Ag injection the presentation of DB06-1 by APC loaded *in vivo* induced a clearly stronger *i*NKT cell response *ex vivo* compared to αGalCer (Fig. 4C). While we did not detect surface Ag-CD1d complexes by flow cytometry on DCs of mice injected 2 h earlier, it is likely that an amount of complexes below the detection limit of flow cytometry was able to give an optimal stimulation of *i*NKT cell hybridomas *in vitro*. It is also possible, however, that some lipid Ag taken up by DCs *in vivo* was able to load into CD1d during the culture period with the *i*NKT cell hybridoma cells. Regardless, our data demonstrate that DB06-1 is taken up and presented more effectively by DCs *in vivo*.

CD1d recycling enhances DB06-1 presentation

Previous data indicated that presentation of Th1 cytokine skewing lipid Ags was increased when CD1d cycled through endosomal compartments. Furthermore, CD1d molecules presenting Th1 skewing Ags were preferentially associated with lipid rafts (21). CD1d contains a tyrosine motif in its cytoplasmic tail that allows trafficking to endosomal compartments. To study the role of endosome trafficking in the presentation of DB06-1, we used transfected cell lines that either expressed WT CD1d or tail-deleted (TD) CD1d lacking the cytoplasmic tail, including the tyrosine motif important for endosomal location. As reference Ag, we used galactosyl (α1–2) galactosyl ceramide (GGC), which is known to require lysosomal processing to cleave the terminal sugar to yield the active compound, αGalCer. Without recycling through endolysosomal compartments, GGC is not recognized by *i*NKT cell hybridomas (54). Like GGC, DB06-1 presentation to an *i*NKT cell hybridoma also was greatly reduced when CD1d lacked the ability to recycle through endosomal compartments as compared to the wild-type CD1d cells (Fig. 5A). In order to confirm that this recycling was also important *in vivo*, we used a mouse strain that lacked the tyrosine motif of the *cd1d* gene (CD1-TD). Although surface expression of CD1d is significantly higher on APCs from CD1-TD mice compared to control mice, *i*NKT cells do not develop to WT numbers in CD1d-TD mice, likely due to the inability of CD1d to acquire the ligands appropriate for *i*NKT cell positive selection (30). To study the capability of APCs from these mice, we injected CD1-TD mice with DB06-1 or αGalCer, isolated splenic $CD11c^+$ cells at 24 h, and used different concentrations of the DCs to stimulate an *i*NKT cell hybridoma *ex vivo* as a readout of Ag presentation. αGalCer was used as the control Ag because although it shows a dependence on CD1d recycling in some experiments, in our experience, it can load effectively into CD1d molecules on the cell surface (54). Although *i*NKT cell response could be elicited by DCs derived from CD1-TD mice that had been injected with DB06-1, this response was reduced compared the one stimulated by DCs from mice injected with αGalCer (Fig. 5B). This profile is opposite to the one obtained when these two Ags were injected into WT mice (Fig. 4D). Together, these data demonstrate that DB06-1 is presented when CD1d traffics normally through late endosomal compartments, and it is more dependent on CD1d recycling than αGalCer.

The iNKT cell TCR has a high affinity for the CD1d-DB06-1 complex

One hypothesis for the ability of Ags to induce a Th1 cytokine-skewed response *in vivo* is that those Ags have an increased affinity for the *i*NKT TCR when bound to CD1d (55). Equilibrium binding analysis using SPR demonstrated a binding affinity (K_D) of the mouse

Vα14Vβ8.2 *i*NKT cell TCR for mouse CD1d-DB06-1 complexes of 56 ± 6 nM (Fig. 6A), approximately 2-fold weaker than the binding affinity observed with αGalCer loaded CD1d (24 nM) (data not shown). The association rate (k_a =5.2 ± 0.7 10^4 M^{-1} s^{-1}) and dissociation rate (k_d=2.9 ± 0.7 10^{-3} s^{-1}) were comparable to the rates for αGalCer (k_a = 7.84 10^4 M^{-1} s^{-1} and k_d = 1.61 10^{-3} s^{-1}, respectively; data not shown).

We also analyzed the affinity of a human autoreactive *i*NKT cell TCR for the human CD1d-DB06-1 complex (Fig. 6B). Using steady state kinetic modeling, whereby we plotted the residual units of the sensorgram against the concentration of the TCR and calculated a line of best fit (Fig. 6C), we determined that the affinity of the autoreactive human TCR for the CD1d-DB06-1 complex (0.485 μM ± 0.265) was again approximately 2-fold weaker than the αGalCer-CD1d complex (0.22 μM ± 0.11). Therefore, we conclude that although the *i*NKT cell TCR has a high affinity for the CD1d-DB06-1 complex, the interaction with the αGalCer-CD1d complexes is even stronger. These results are consistent with other data demonstrating that increased TCR affinity cannot explain increased Th1 cytokine release resulting from *i*NKT cell stimulation.

Structure of the mouse TCR-DB06-1-CD1d ternary complex

In order to characterize the biochemical features of the binding of the DB06-1 GSL to CD1d and the *i*NKT TCR, we determined the structure of the ternary complex by X-ray crystallography (Fig. 7A and Supplemental Table I). The complex crystallized in the space group $C222_1$, with one complex in the asymmetric unit. The binding orientation of the *i*NKT cell TCR is consistent with the conserved parallel docking mode previously described (56). The TCR docks over the CD1d antigen binding groove in an orientation that is markedly different than the diagonal binding footprint seen in MHC-peptide-TCR complexes. As previously shown with models using the same TCR construct (53), the TCR interacts with CD1d using amino acids in the TCR CDR3α and CDR2β loops as well as a CDR3β-dependent contact (Fig. 7B). The same previously seen polar contacts are also formed between the α chain (N30, R95, G96) of the *i*NKT TCR and the DB06-1 Ag (Fig. 7B). There is well-defined density for the DB06-1 ligand (Fig. 7C), with the galactose head group exposed to recognition by the *i*NKT cell TCR. Polar contacts between the GSL Ag and amino acids E80, E153, and T156 of CD1d are virtually identical to the interactions of CD1d with αGalCer. The binding of orientation of DB06-1 within the hydrophobic A′ and F ′ grooves of CD1d is also conserved, with the acyl chain localizing to the A′ groove and the sphingoid base to the F′ groove, with minimal to no differences when superimposed on the αGalCer-CD1d structure (data not shown). Because the two molecules are chemically similar in these regions, this similarity was expected. DB06-1 differs from αGalCer by the replacement of an oxygen with a sulfur. The sulfur atom, which is 50% bigger than the oxygen atom present in αGalCer (Fig. 7D) took up more space in CD1d (Fig. 7E), possibly forming more intimate contacts with the surrounding CD1d residues.

DB06-1 induces IL-10

Recent studies have identified an *i*NKT cell subset, which we called NKT10 cells, that produces IL-10 and which may have regulatory function (12, 57). Previous experiments demonstrated that *i*NKT cells exposed to αGalCer *in vivo* were more capable of producing

IL-10 when re-stimulated weeks to months later. In order to compare a strongly Th-1 biasing GSL Ag to αGalCer for the induction NKT10 cells, we injected mice with DB06-1 or αGalCer, and four weeks later measured the capacity for splenic *i*NKT cells to produce IL-10 following a brief stimulation *in vitro* with PMA and ionomycin followed by intracellular cytokine staining. Remarkably, the frequency of IL-10$^+$ *i*NKT cells one month after DB06-1 immunization was significantly larger than after αGalCer immunization (Fig. 8). A similar enhancement of IL-10 production was observed after immunization with DB06-1 when the *i*NKT cells were re-stimulated with Ag one month later (data not shown). These data suggest a possible link between a strong Th1 cytokine response and the induction of IL-10 producing *i*NKT cells.

Discussion

Understanding how structural changes in GSL Ags can differentially modulate the immune response is important, not only for understanding how *i*NKT cells influence immunity, but also for developing therapeutic GSLs. For example, Ags that preferentially skew the immune response towards Th1 cytokine production could be useful as vaccine adjuvants and anti-cancer therapeutics (58, 59). Here we have characterized DB06-1, a GSL Ag that differs from the well-studied αGalCer by only a single atom. Despite this subtle change, we show that DB06-1 leads to changes in the immune system of mice that are more pronounced than those induced by αGalCer. Within one day after immunization, DB06-1 caused an increased Th1-cytokine response, and on the long-term it induced more NKT10 cells when compared to αGalCer. Moreover, because DB06-1 can activate human *i*NKT cells it, or related antigens with thioamide groups, could be therapeutically relevant. It is noteworthy that DB06-1 was not better or markedly different from αGalCer using *in vitro* assays, considering not only TCR binding to the GSL-CD1d complex, but also activation *in vitro* using CD1d-coated plates or APCs. In almost all the *in vivo* assays, however, it was superior, including increased loading onto DCs *in vivo*, increased IFN-γ in the serum, augmented IL-12 in the serum, and increased NK cell IFN-γ production. These findings emphasize the complexity of assaying GSL Ag efficacy, and the need to study these compounds *in vivo*.

A number of theories have been proposed for Th1 cytokine skewing following GSL Ag immunization, but despite much effort and investigation, this process remains incompletely understood. Selective uptake and presentation by an APC type, for example DC versus B lymphocytes could be important (60), although recent evidence indicates that CD8α$^+$ DC are the most essential APCs for the presentation of injected lipid Ags, regardless if they are Th1 or Th2 skewing (51). The effect of a GSL Ag on the APC could be critical, perhaps a result of its trafficking in the cell and the site where it is loaded into CD1d. In fact, Th1 cytokine skewing has been associated with a requirement for Ag internalization for loading into CD1d, as opposed to loading into CD1d on the cell surface (61). This type of immune response is also correlated with appearance of GSL-CD1d complexes on the cell surface in detergent resistant domains (21). Consistent with this, DB06-1 was originally identified in a screen of lipid Ags that were associated with detergent resistant domains when bound to CD1d. Furthermore, this Ag was previously shown to stimulate robust IFN-γ production *in vivo*, but cytokine production in response to it was not compared to αGalCer, which could

be classified as a Th0 Ag, considering the ratio of IL-4 to IFN-γ that it induces (21). For unknown reasons, the different trafficking of GSLs in APC are linked to changes in the DC, such as increased expression of CD86, that help to stimulate Th1 responses.

Another theory for Th1 cytokine skewing proposes that IFN-γ production is a result of prolonged stimulation by GSL-CD1d complexes, which could be due to increased TCR affinity, increased stability of GSL-CD1d complexes, or pharmacokinetic properties. For example, a decreased rate of compound degradation, as originally proposed for C-glycoside, could contribute to prolonged *i*NKT cell stimulation. In fact, our data indicate that several Th1 skewing GSL Ags have an increased half-life *in vivo* as Ag- CD1d complexes on the surface of APCs (13, 53). Furthermore, the results from structural studies indicate that some Th1 skewing glycolipids may have increased contacts with CD1d, and this enhanced interaction with CD1d that may contribute to the prolonged antigenic stimulation (53, 62). Although these different theories have merit, one class of theory alone probably does not account for all compounds that cause Th1 biasing cytokine release, and these mechanisms are not mutually exclusive.

The novel compound characterized here fits with several of the theories and mechanisms described above for the activity of Ags that cause Th1 biased cytokine responses. For example, DB06-1 is preferentially presented by $CD11c^+$ DCs to *i*NKT cells. As previously mentioned, it was known that DB06-1 bound to CD1d localized to detergent resistant domains (21). Moreover, DB06-1 also shows a strong preference for internalization by APCs for effective presentation. Although DB06-1 can be loaded into CD1d *in vitro* in a cell free assay, optimal presentation of this lipid is achieved by recycling through endosomal compartments. While DB06-1 has a slightly weaker TCR affinity when presented by CD1d than αGalCer, this is not surprising as it has been observed with other Th1 biasing GSL Ags, including the most well-studied Ag, C-glycoside (13). Similar to other Th1 biasing *i*NKT cell GSL Ags (53), DB06-1 does persist as GSL-CD1d complexes on DCs *in vivo* as measured by the ability of ex vivo DCs to activate an *i*NKT cell hybridoma. When DCs from mice injected with DB06-1 were analyzed ex vivo, they were more effective at stimulating the iNKT cell hybridoma at both the early (2 h) and late (24 h) time points, demonstrating increased loading into the CD1d groove *in vivo*. Consistent with this, we also observed increased Ag-CD1d complexes by flow cytometry but only at 24 h, likely because the increased epitope density at the earlier times was not sufficient to be detected by flow cytometry. We therefore propose that although the larger sulfur atom may make CD1d loading more difficult *in vitro* in a cell free assay, this may be overcome in the presence of lipid transfer proteins in the lysosome. Conversely, the sulfur atom also may allow for better locking within the CD1d groove, inhibiting the GSL Ag from replacement. Furthermore, sulfur is also less electronegative than oxygen, and this may allow DB06-1 to be maintained in the CD1d hydrophobic pocket longer. Therefore we speculate that as for other Th1 biasing *i*NKT cells Ags, the enhanced molecular interaction of DB06-1 with CD1d will permit an increased and prolonged *i*NKT cell stimulation that leads to increased IFN-γ production by *trans*-activated NK cells.

A population of *i*NKT cells that produce IL-10, called NKT10 cells, has recently been described (12, 57). These NKT10 cells are induced or expand greatly after a strong antigenic

stimulation, for example after αGalCer immunization, they are long-lived and they preferentially localize to adipose tissue. An intriguing property of DB06-1 described here is the robust IL-10 production by *i*NKT cells from mice injected with this compound one month earlier when compared to those injected with αGalCer. We have made a similar observation of increased IL-10 production when *i*NKT cells were re-stimulated weeks after injection with several other Th1-biasing GSL Ags (manuscript in preparation), suggesting this property could be a more general one. This effect, extending far beyond the initial IFN-γ burst, could have profound implications regarding the development of *i*NKT cell GSL Ags as therapeutics. Previous studies have shown that mice pretreated with αGalCer have a decreased ability to reject tumors due to the IL-10 production by NKT10 cells (12). If we extrapolate, it is possible that a GSL that leads to a more pronounced IL-10 response would theoretically lead to less tumor rejection and would thus be a poor target for a cancer therapeutic. However, other diseases may benefit from activation of NKT10 cells. Repetitive αGalCer injections have been shown to lead to a reduced disease score in a mouse model of multiple sclerosis. This protection has been suggested to be correlated with the ability of αGalCer to induce NKT10 cell IL-10 production as IL-$10^{-/-}$ mice are not protected (63). Single injections of αGalCer are unable to lead to this protection (64), however, a strong IL-10 inducing GSL like DB06-1 may prove to be more effective, and IFN-γ is known to be necessary to promote this response (65). In addition with this, αGalCer has been shown to be protective in a mouse rheumatoid arthritis model through an IL-10 mediated response (66). Although humans have NKT10 cells, it is unknown if the profound response seen in mice will be found in humans and more studies are needed to address the implications of IL-10 producing NKT10 cells on human therapeutics.

In summary, DB06-1 is a powerful activating GSL Ag capable of impacting the mouse immune system days and weeks after immunization. Its chemical properties allow for stable formation of complexes with CD1d when it can be internalized within DCs *in vivo*. The characterization of this GSL, along with previous *i*NKT cell GSL Ags, contributes to our understanding of the mechanisms for diverse *i*NKT cell influences on the immune response and will aid in the logical design of potential future *i*NKT cell GSL Ag therapeutics.

Supplementary Material

Refer to Web version on PubMed Central for supplementary material.

Acknowledgments

The authors wish to thank Dr. Jamie Rossjohn for the autoreactive human TCR plasmid, Dr. Albert Bendelac for the CD1-TD mice, and Kyowa Hakko Kirin Co. Ltd. for αGalCer. The authors would also like to thank the Stanford Synchrotron Radiation Laboratory, the Flow Cytometry Core Facility and the Department of Laboratory Animal Care at the La Jolla Institute for Allergy and Immunology for excellent technical assistance.

Funding: AI45053 (MK), AI71922 (MK), UCSD Rheumatology T32 grant (MZ), AI074952 (DMZ), AI107318 (DMZ), AI091987 (WY) and AI45889 (SAP).

Abbreviations

αGalCer	alpha-galactosylceramide

B6	C57BL/6 mouse strain
CD1d-WT A20	transfected B cell line expressing CD1d
CD1d-TD A20	transfected B cell line expressing CD1d lacking a tyrosine motif in its cytoplasmic tail
DC	dendritic cell
GGC	galactosyl (α1–2) galactosyl ceramide
GSL	glycosphingolipid
ICCS	intracellular cytokine staining
NKT	Natural Killer T cell
o/n	overnight
SPR	surface plasmon resonance
TD	tail deleted
WT	wild type

References

1. Berzins SP, Smyth MJ, Baxter AG. Presumed guilty: natural killer T cell defects and human disease. Nature Reviews Immunology. 2011; 11:131–142.
2. MacDonald HR, Mycko MP. Development and selection of Valpha l4i NKT cells. Curr Top Microbiol Immunol. 2007; 314:195–212. [PubMed: 17593662]
3. Barral DC, Brenner MB. CD1 antigen presentation: how it works. Nature Reviews Immunology. 2007; 7:929–941.
4. Zajonc DM, Cantu C, Mattner J, Zhou D, Savage PB, Bendelac A, Wilson IA, Teyton L. Structure and function of a potent agonist for the semi-invariant natural killer T cell receptor. Nat Immunol. 2005; 6:810–818. [PubMed: 16007091]
5. Borg NA, Wun KS, Kjer-Nielsen L, Wilce MCJ, Pellicci DG, Koh R, Besra GS, Bharadwaj M, Godfrey DI, McCluskey J, Rossjohn J. CD1d-lipid-antigen recognition by the semi-invariant NKT T-cell receptor. Nature. 2007; 448:44–49. [PubMed: 17581592]
6. Lantz O, Bendelac A. An invariant T cell receptor alpha chain is used by a unique subset of major histocompatibility complex class I-specific CD4+ and CD4-8- T cells in mice and humans. Journal of Experimental Medicine. 1994; 180:1097–1106. [PubMed: 7520467]
7. Morita M, Motoki K, Akimoto K, Natori T, Sakai T, Sawa E, Yamaji K, Koezuka Y, Kobayashi E, Fukushima H. Structure-activity relationship of alpha-galactosylceramides against B16-bearing mice. J Med Chem. 1995; 38:2176–2187. [PubMed: 7783149]
8. Spada FM, Koezuka Y, Porcelli SA. CD1d-restricted Recognition of Synthetic Glycolipid Antigens by Human Natural Killer T Cells. The Journal of Experimental Medicine. 1998; 188:1529–1534. [PubMed: 9782130]
9. Bendelac A, Savage PB, Teyton L. The Biology of NKT Cells. Annu Rev Immunol. 2007; 25:297–336. [PubMed: 17150027]
10. Parekh VV, Wilson MT, Olivares-Villagómez D, Singh AK, Wu L, Wang CR, Joyce S, Van Kaer L. Glycolipid antigen induces long-term natural killer T cell anergy in mice. J Clin Invest. 2005; 115:2572–2583. [PubMed: 16138194]
11. Sullivan BA, Kronenberg M. Activation or anergy: NKT cells are stunned by alpha-galactosylceramide. J Clin Invest. 2005; 115:2328–2329. [PubMed: 16138189]

12. Sag D, Krause P, Hedrick CC, Kronenberg M, Wingender G. IL-10-producing NKT10 cells are a distinct regulatory invariant NKT cell subset. J Clin Invest. 2014; 124:3725–3740. [PubMed: 25061873]
13. Sullivan BA, Nagarajan NA, Wingender G, Wang J, Scott I, Tsuji M, Franck RW, Porcelli SA, Zajonc DM, Kronenberg M. Mechanisms for glycolipid antigen-driven cytokine polarization by Valpha14i NKT cells. J Immunol. 2010; 184:141–153. [PubMed: 19949076]
14. Smyth MJ, Crowe NY, Pellicci DG, Kyparissoudis K, Kelly JM, Takeda K, Yagita H, Godfrey DI. Sequential production of interferon-gamma by NK1.1(+) T cells and natural killer cells is essential for the antimetastatic effect of alpha-galactosylceramide. Blood. 2002; 99:1259–1266. [PubMed: 11830474]
15. Yu KOA, Porcelli SA. The diverse functions of CD1d-restricted NKT cells and their potential for immunotherapy. Immunol Lett. 2005; 100:42–55. [PubMed: 16083968]
16. Brennan PJ, Brigl M, Brenner MB. Invariant natural killer T cells: an innate activation scheme linked to diverse effector functions. Nature Reviews Immunology. 2013; 13:101–117.
17. Schneiders FL, Scheper RJ, von Blomberg BME, Woltman AM, Janssen HLA, van den Eertwegh AJM, Verheul HMW, de Gruijl TD, van der Vliet HJ. Clinical experience with α-galactosylceramide (KRN7000) in patients with advanced cancer and chronic hepatitis B/C infection. Clinical Immunology. 2011; 140:130–141. [PubMed: 21169066]
18. Terabe M, Berzofsky JA. The role of NKT cells in tumor immunity. Adv Cancer Res. 2008; 101:277–348. [PubMed: 19055947]
19. Franck RW, Tsuji M. α-C-Galactosylceramides: Synthesis and Immunology. Acc Chem Res. 2006; 39:692–701. [PubMed: 17042469]
20. Patel O, Cameron G, Pellicci DG, Liu Z, Byun HS, Beddoe T, McCluskey J, Franck RW, Castaño AR, Harrak Y, Llebaria A, Bittman R, Porcelli SA, Godfrey DI, Rossjohn J. NKT TCR Recognition of CD1d- -C-Galactosylceramide. The Journal of Immunology. 2011; 187:4705–4713. [PubMed: 21964029]
21. Arora P, Venkataswamy MM, Baena A, Bricard G, Li Q, Veerapen N, Ndonye R, Park JJ, Lee JH, Seo KC, Howell AR, Chang YT, Illarionov PA, Besra GS, Chung SK, Porcelli SA. A Rapid Fluorescence-Based Assay for Classification of iNKT Cell Activating Glycolipids. J Am Chem Soc. 2011; 133:5198–5201. [PubMed: 21425779]
22. Yu KOA, Im JS, Molano A, Dutronc Y, Illarionov PA, Forestier C, Fujiwara N, Arias I, Miyake S, Yamamura T, Chang YT, Besra GS, Porcelli SA. Modulation of CD1d-restricted NKT cell responses by using N-acyl variants of alpha-galactosylceramides. Proc Natl Acad Sci USA. 2005; 102:3383–3388. [PubMed: 15722411]
23. Naidenko OV, Maher JK, Ernst WA, Sakai T, Modlin RL, Kronenberg M. Binding and antigen presentation of ceramide-containing glycolipids by soluble mouse and human CD1d molecules. Journal of Experimental Medicine. 1999; 190:1069–1080. [PubMed: 10523605]
24. Sidobre S, Hammond KJL, Bénazet-Sidobre L, Maltsev SD, Richardson SK, Ndonye RM, Howell AR, Sakai T, Besra GS, Porcelli SA, Kronenberg M. The T cell antigen receptor expressed by Valpha14i NKT cells has a unique mode of glycosphingolipid antigen recognition. Proceedings of the National Academy of Sciences. 2004; 101:12254–12259.
25. Tupin E, Kronenberg M. Activation of natural killer T cells by glycolipids. Meth Enzymol. 2006; 417:185–201. [PubMed: 17132506]
26. Brossay L, Tangri S, Bix M, Cardell S, Locksley R, Kronenberg M. Mouse CD1-autoreactive T cells have diverse patterns of reactivity to CD1+ targets. The Journal of Immunology. 1998; 160:3681–3688. [PubMed: 9558068]
27. Inaba, K.; Swiggard, WJ.; Steinman, RM.; Romani, N.; Schuler, G.; Brinster, C. Isolation of Dendritic Cells. John Wiley & Sons, Inc; Hoboken, NJ, USA: 2009. p. 3.7.1-3.7.19.
28. Lawton AP, Prigozy TI, Brossay L, Pei B, Khurana A, Martin D, Zhu T, Späte K, Ozga M, Höning S, Bakke O, Kronenberg M. The mouse CD1d cytoplasmic tail mediates CD1d trafficking and antigen presentation by adaptor protein 3-dependent and -independent mechanisms. The Journal of Immunology. 2005; 174:3179–3186. [PubMed: 15749847]

29. Rogers PR, Matsumoto A, Naidenko O, Kronenberg M, Mikayama T, Kato S. Expansion of human Valpha24+ NKT cells by repeated stimulation with KRN7000. Journal of Immunological Methods. 2004; 285:197–214. [PubMed: 14980434]
30. Chiu YH, Park SH, Benlagha K, Forestier C, Jayawardena-Wolf J, Savage PB, Teyton L, Bendelac A. Multiple defects in antigen presentation and T cell development by mice expressing cytoplasmic tail–truncated CD1d. Nat Immunol. 2001; 3:55–60. [PubMed: 11731798]
31. Caton ML, Smith-Raska MR, Reizis B. Notch–RBP-J signaling controls the homeostasis of CD8– dendritic cells in the spleen. The Journal of Experimental Medicine. 2007; 204:1653–1664. [PubMed: 17591855]
32. Wen X, Rao P, Carreño LJ, Kim S, Lawrenczyk A, Porcelli SA, Cresswell P, Yuan W. Human CD1d knock-in mouse model demonstrates potent antitumor potential of human CD1d-restricted invariant natural killer T cells. Proc Natl Acad Sci USA. 2013; 110:2963–2968. [PubMed: 23382238]
33. Capone M, Cantarella D, Schümann J, Naidenko OV, Garavaglia C, Beermann F, Kronenberg M, Dellabona P, MacDonald HR, Casorati G. Human invariant V alpha 24-J alpha Q TCR supports the development of CD1d-dependent NK1.1+ and NK1.1- T cells in transgenic mice. The Journal of Immunology. 2003; 170:2390–2398. [PubMed: 12594262]
34. Tyznik AJ, Tupin E, Nagarajan NA, Her MJ, Benedict CA, Kronenberg M. Cutting edge: the mechanism of invariant NKT cell responses to viral danger signals. J Immunol. 2008; 181:4452–4456. [PubMed: 18802047]
35. Matsuda JL, Naidenko O, Gapin L, Nakayama T, Taniguchi M, Wang CR, Koezuka Y, Kronenberg M. Tracking the Response of Natural Killer T Cells to a Glycolipid Antigen Using Cd1d Tetramers. Journal of Experimental Medicine. 2000; 192:741–754. [PubMed: 10974039]
36. Zajonc DM, Maricic I, Wu D, Halder R, Roy K, Wong C-H, Kumar V, Wilson IA. Structural basis for CD1d presentation of a sulfatide derived from myelin and its implications for autoimmunity. Journal of Experimental Medicine. 2005; 202:1517–1526. [PubMed: 16314439]
37. Wang J, Li Y, Kinjo Y, Mac TT, Gibson D, Painter GF, Kronenberg M, Zajonc DM. Lipid binding orientation within CD1d affects recognition of Borrelia burgorferi antigens by NKT cells. Proceedings of the National Academy of Sciences. 2010; 107:1535–1540.
38. Matulis G, Sanderson JP, Lissin NM, Asparuhova MB, Bommineni GR, Schümperli D, Schmidt RR, Villiger PM, Jakobsen BK, Gadola SD. Innate-like control of human iNKT cell autoreactivity via the hypervariable CDR3beta loop. PLoS Biol. 2010; 8:1–12.
39. Pellicci DG, Clarke AJ, Patel O, Mallevaey T, Beddoe T, Le Nours J, Uldrich AP, McCluskey J, Besra GS, Porcelli SA, Gapin L, Godfrey DI, Rossjohn J. Recognition of β-linked self glycolipids mediated by natural killer T cell antigen receptors. Nat Immunol. 2011; 12:827–833. [PubMed: 21804559]
40. Gadola SD. Structure and binding kinetics of three different human CD1d-alpha-galactosylceramide-specific T cell receptors. Journal of Experimental Medicine. 2006; 203:699–710. [PubMed: 16520393]
41. Leslie AGW. The integration of macromolecular diffraction data. Acta Crystallogr D Biol Crystallogr. 2006; 62:48–57. [PubMed: 16369093]
42. Zajonc DM, Savage PB, Bendelac A, Wilson IA, Teyton L. Crystal Structures of Mouse CD1d-iGb3 Complex and its Cognate Vα14 T Cell Receptor Suggest a Model for Dual Recognition of Foreign and Self Glycolipids. Journal of Molecular Biology. 2008; 377:1104–1116. [PubMed: 18295796]
43. Aspeslagh S, Li Y, Yu ED, Pauwels N, Trappeniers M, Girardi E, Decruy T, Van Beneden K, Venken K, Drennan M, Leybaert L, Wang J, Franck RW, Van Calenbergh S, Zajonc DM, Elewaut D. Galactose-modified iNKT cell agonists stabilized by an induced fit of CD1d prevent tumour metastasis. EMBO J. 2011; 30:2294–2305. [PubMed: 21552205]
44. Emsley P, Lohkamp B, Scott WG, Cowtan K. Features and development of Coot. Acta Crystallogr D Biol Crystallogr. 2010; 66:486–501. [PubMed: 20383002]
45. Lovell SC I, Davis W, Arendall WB, de Bakker PIW, Word JM, Prisant MG, Richardson JS, Richardson DC. Structure validation by Calpha geometry: phi,psi and Cbeta deviation. Proteins. 2003; 50:437–450. [PubMed: 12557186]

46. Carnaud C, Lee D, Donnars O, Park SH, Beavis A, Koezuka Y, Bendelac A. Cutting edge: Cross-talk between cells of the innate immune system: NKT cells rapidly activate NK cells. The Journal of Immunology. 1999; 163:4647–4650. [PubMed: 10528160]
47. Kawakami K, Kinjo Y, Yara S, Koguchi Y, Uezu K, Nakayama T, Taniguchi M, Saito A. Activation of Valpha14(+) natural killer T cells by alpha-galactosylceramide results in development of Th1 response and local host resistance in mice infected with Cryptococcus neoformans. Infection and Immunity. 2001; 69:213–220. [PubMed: 11119508]
48. Kitamura H, Iwakabe K, Yahata T, Nishimura S, Ohta A, Ohmi Y, Sato M, Takeda K, Okumura K, Van Kaer L, Kawano T, Taniguchi M, Nishimura T. The natural killer T (NKT) cell ligand alpha-galactosylceramide demonstrates its immunopotentiating effect by inducing interleukin (IL)-12 production by dendritic cells and IL-12 receptor expression on NKT cells. Journal of Experimental Medicine. 1999; 189:1121–1128. [PubMed: 10190903]
49. Parekh VV, Singh AK, Wilson MT, Olivares-Villagómez D, Bezbradica JS, Inazawa H, Ehara H, Sakai T, Serizawa I, Wu L, Wang CR, Joyce S, Van Kaer L. Quantitative and qualitative differences in the in vivo response of NKT cells to distinct alpha- and beta-anomeric glycolipids. The Journal of Immunology. 2004; 173:3693–3706. [PubMed: 15356115]
50. Tyznik AJ, Verma S, Wang Q, Kronenberg M, Benedict CA. Distinct Requirements for Activation of NKT and NK Cells during Viral Infection. The Journal of Immunology. 2014; 192:3676–3685. [PubMed: 24634489]
51. Arora P, Baena A, Yu KOA, Saini NK, Kharkwal SS, Goldberg MF, Kunnath-Velayudhan S, Carreño LJ, Venkataswamy MM, Kim J, Lazar-Molnar E, Lauvau G, Chang YT, Liu Z, Bittman R, Al-Shamkhani A, Cox LR, Jervis PJ, Veerapen N, Besra GS, Porcelli SA. A Single Subset of Dendritic Cells Controls the Cytokine Bias of Natural Killer T Cell Responses to Diverse Glycolipid Antigens. Immunity. 2014; 40:105–116. [PubMed: 24412610]
52. Barral P, Polzella P, Bruckbauer A, van Rooijen N, Besra GS, Cerundolo V, Batista FD. CD169(+) macrophages present lipid antigens to mediate early activation of iNKT cells in lymph nodes. Nat Immunol. 2010; 11:303–312. [PubMed: 20228797]
53. Tyznik AJ, Farber E, Girardi E, Birkholz A, Li Y, Chitale S, So R, Arora P, Khurana A, Wang J, Porcelli SA, Zajonc DM, Kronenberg M, Howell AR. Glycolipids that Elicit IFN-γ-Biased Responses from Natural Killer T Cells. Chem Biol. 2011; 18:1620–1630. [PubMed: 22195564]
54. Prigozy TI, Naidenko OV, Qasba P, Elewaut D, Brossay L, Khurana A, Natori T, Koezuka Y, Kulkarni AB, Kronenberg M. Glycolipid Antigen Processing for Presentation by CD1d Molecules. Science. 2001; 291:664–667. [PubMed: 11158680]
55. Oki S, Chiba A, Yamamura T, Miyake S. The clinical implication and molecular mechanism of preferential IL-4 production by modified glycolipid-stimulated NKT cells. J Clin Invest. 2004; 113:1631–1640. [PubMed: 15173890]
56. Rossjohn J, Pellicci DG, Patel O, Gapin L, Godfrey DI. Recognition of CD1d-restricted antigens by natural killer T cells. Nature Reviews Immunology. 2012; 12:845–857.
57. Lynch L, Michelet X, Zhang S, Brennan PJ, Moseman A, Lester C, Besra G, Vomhof-Dekrey EE, Tighe M, Koay H-F, Godfrey DI, Leadbetter EA, Sant'Angelo DB, von Andrian U, Brenner MB. Regulatory iNKT cells lack expression of the transcription factor PLZF and control the homeostasis of Treg cells and macrophages in adipose tissue. Nat Immunol. 2015; 16:85–95. [PubMed: 25436972]
58. Padte NN, Boente-Carrera M, Andrews CD, McManus J, Grasperge BF, Gettie A, Coelho-dos-Reis JG, Li X, Wu D, Bruder JT, Sedegah M, Patterson N, Richie TL, Wong C-H, Ho DD, Vasan S, Tsuji M. A Glycolipid Adjuvant, 7DW8-5, Enhances CD8+ T Cell Responses Induced by an Adenovirus-Vectored Malaria Vaccine in Non-Human Primates. PLoS ONE. 2013; 8:1–11.
59. Uchida T, Horiguchi S, Tanaka Y, Yamamoto H, Kunii N, Motohashi S, Taniguchi M, Nakayama T, Okamoto Y. Phase I study of α-galactosylceramide-pulsed antigen presenting cells administration to the nasal submucosa in unresectable or recurrent head and neck cancer. Cancer Immunol Immunother. 2008; 57:337–345. [PubMed: 17690880]
60. Bai L, Constantinides MG, Thomas SY, Reboulet R, Meng F, Koentgen F, Teyton L, Savage PB, Bendelac A. Distinct APCs Explain the Cytokine Bias of -Galactosylceramide Variants In Vivo. The Journal of Immunology. 2012; 188:3053–3061. [PubMed: 22393151]

61. Lalazar G, Ben Yáacov A, Eliakim-Raz N, Livovsky DM, Pappo O, Preston S, Zolotarov L, Ilan Y. Beta-glycosphingolipids-mediated lipid raft alteration is associated with redistribution of NKT cells and increased intrahepatic CD8+ T lymphocyte trapping. J Lipid Res. 2008; 49:1884–1893. [PubMed: 18480029]

62. Aspeslagh S, Nemcovic M, Pauwels N, Venken K, Wang J, Van Calenbergh S, Zajonc DM, Elewaut D. Enhanced TCR Footprint by a Novel Glycolipid Increases NKT-dependent Tumor Protection. J Immunol. 2013; 191:2916–2925. [PubMed: 23960235]

63. Singh AK, Wilson MT, Hong S, Olivares-Villagomez D, Du C, Stanic AK, Joyce S, Sriram S, Koezuka Y, Van Kaer L. Natural killer T cell activation protects mice against experimental autoimmune encephalomyelitis. Journal of Experimental Medicine. 2001; 194:1801–1811. [PubMed: 11748281]

64. Jahng AW, Maricic I, Pedersen B, Burdin N, Naidenko O, Kronenberg M, Koezuka Y, Kumar V. Activation of natural killer T cells potentiates or prevents experimental autoimmune encephalomyelitis. Journal of Experimental Medicine. 2001; 194:1789–1799. [PubMed: 11748280]

65. Furlan R, Bergami A, Cantarella D, Brambilla E, Taniguchi M, Dellabona P, Casorati G, Martino G. Activation of invariant NKT cells by alphaGalCer administration protects mice from MOG35-55-induced EAE: critical roles for administration route and IFN-gamma. European Journal of Immunology. 2003; 33:1830–1838. [PubMed: 12811843]

66. Miellot A, Zhu R, Diem S, Boissier MC, Herbelin A, Bessis N. Activation of invariant NK T cells protects against experimental rheumatoid arthritis by an IL-10-dependent pathway. European Journal of Immunology. 2005; 35:3704–3713. [PubMed: 16304639]

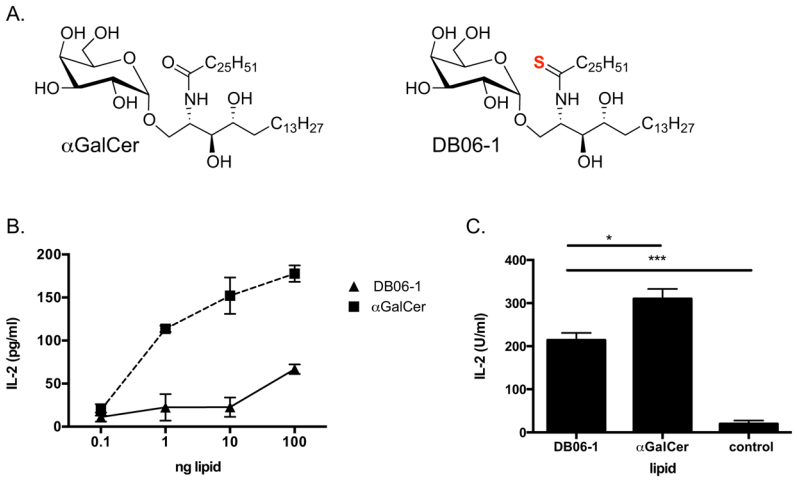

FIGURE 1. DB06-1 is recognized by mouse *i*NKT cells

(A) Chemical structures of αGalCer and DB06-1 are depicted, with the sulfur atom that differentiates DB06-1 shown in red. (B) CD1d coated plate assay whereby soluble CD1d bound to a plate was incubated with the indicated Ags o/n. The 1.2 Vα14 *i*NKT cell hybridoma was added, and IL-2 was measured after 16 h by ELISA to assess TCR engagement. Data are representative of one of two independent experiments. Error bars represent ± SEM of three wells per condition. (C) Bone marrow DCs were incubated with 100 ng/mL lipid Ag o/n and were then co-cultured with 1.2 Vα14 *i*NKT hybridoma cells o/n. Secreted IL-2 was measured the following day by ELISA to asses hybridoma stimulation. Data are from one representative of two independent experiments. Error bars represent ± SEM of three wells per condition.

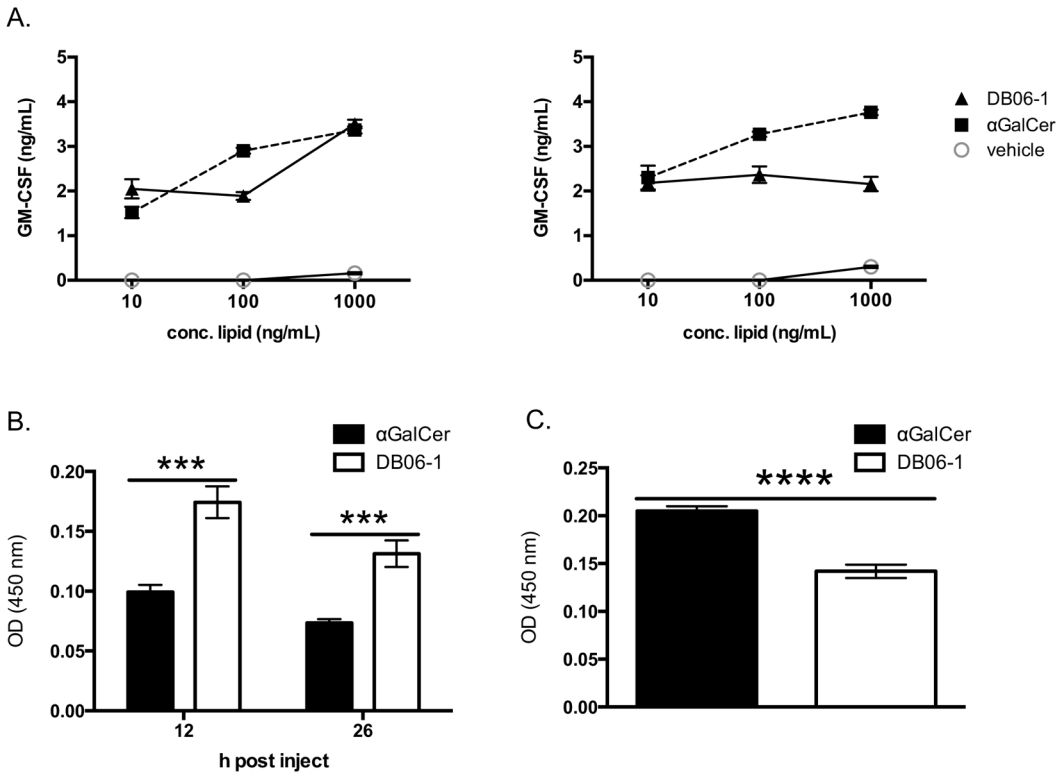

FIGURE 2. DB06-1 is recognized by human *i*NKT cells

(A) Two human *i*NKT cell lines were stimulated o/n with PBMCs that had been pulsed for 16 h with the indicated Ag concentrations. ELISA for GM-CSF was used as a readout of *i*NKT cell activation. Data are representative from one of two independent experiments. Error bars represent ± SEM of three wells per condition. (B, C) *i*NKT cell humanized mice (hCD1d x Vα24 Tg) were injected with 1 μg of GSL Ag. At 12 and 26 h post injection, serum IFN-γ cytokine levels were assessed by ELISA (B) and at 2 h serum IL-4 was assessed by ELISA (C).

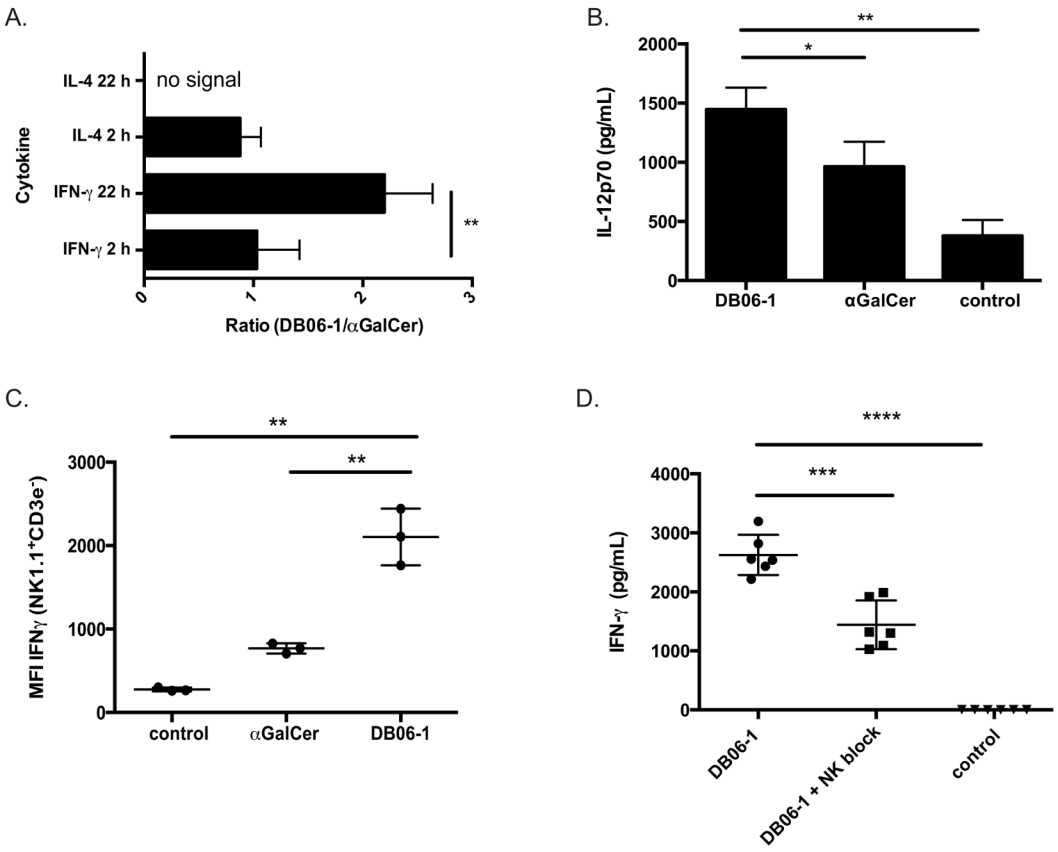

FIGURE 3. Th1 cytokine skewing depends on IL-12 and NK cells

(A) Ratio (DB06-1/αGalCer) of 2 and 22 h cytokine concentrations in sera obtained from C57BL/6 mice after i.v. injection of 1 μg lipid either DB06-1 or αGalCer as measured by ELISA. Data are combination of four independent experiments. Error bars represent ± SEM. (B) IL-12p70 measured by ELISA in sera from C57BL/6 mice injected i.v. with 1 μg of αGalCer or DB06-1 compared to uninjected control mice at 6 h post injection. Data are representative of mouse triplicates for each group for one of two independent experiments. Error bars represent ± SEM. (C) NK cell IFN-γ production from C57BL/6 mice injected iv with 1 μg DB06-1. Splenocytes from DB06-1 or αGalCer injected mice and controls were isolated and cultured in complete media containing GolgiPlug (BD Biosciences) for 4 h. NK cells were gated as live, $B220^{-}$ $NK1.1^{+}$ $CD3\varepsilon^{-}$ cells. The total ICCS IFN-γ MFI of NK cells is plotted. Data are representative of mouse triplicates for each group from one of three independent experiments. Error bars represent ± SEM. (D) IFN-γ in the sera as measured by ELISA at 24 h post injection of DB06-1 of C57BL/6 mice depleted of NK cells with Anti-Asialo-GM1Ab (NK block) were compared to controls. Data are representative of mouse triplicates for each group for one of two independent experiments. Error bars represent ± SEM.

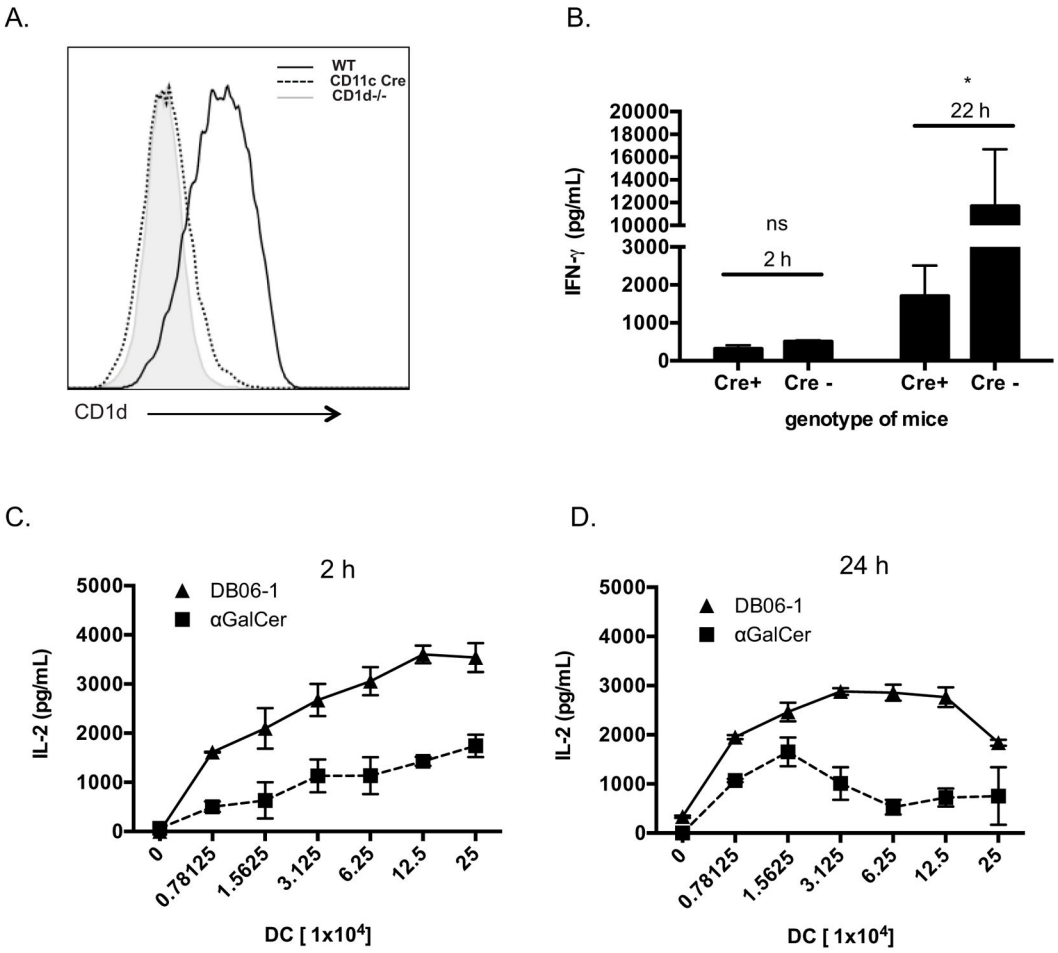

FIGURE 4. Enhanced presentation of DB06-1 by DCs

(A) CD1d deletion in $CD11c^+$ cells in *Cd1d*$^{fl/fl}$ x *Cd11c-Cre* mice. Analysis of gated live, $B220^-$, $TCR\beta^-$, $CD11c^+$ cells from wild type (WT), *Cd1d*$^{fl/fl}$ x *Cd11c-Cre* (CD11c Cre), *and* *Cd1d*$^{-/-}$ ($CD1d^{-/-}$) mice are shown. (B) *Cd1d*$^{fl/fl}$ mice x *Cd11c-Cre* (Cre+) and littermate *Cd1d*$^{fl/fl}$ controls (Cre^-) were injected with 1 μg DB06-1 and were bled at 2 and 22 h and serum IFN-γ was measured by ELISA. Data are representative from one of two independent experiments. Error bars represent ± SEM of at least two mice per condition. (C, D) Ex vivo antigen presentation assay. C57BL/6 mice were injected with 1 μg of the indicated glycolipid and $CD11c^+$ splenic DCs were enriched using magnetic bead isolation at 2 h (C) and 24 h (D) post injection. Indicated numbers of enriched DCs were cultured with 1.2 Vα14 *i*NKT hybridoma cells overnight and IL-2 in the supernatant was measured by ELISA. Data are plotted as the number of enriched DCs per well versus IL-2 (pg/ml). Data are representative of mouse triplicates for each group for one of three independent experiments. Error bars represent ± SEM.

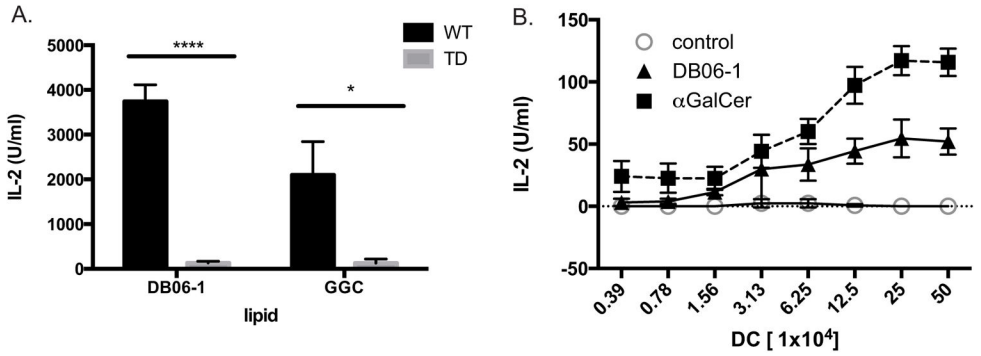

FIGURE 5. Presentation of DB06-1 is enhanced by endolysosomal localization

(A) Antigen presenting A20 cells expressing wild-type (WT) or tail-deleted (TD) CD1d were pulsed with 0.1 ng DB06-1 or 100 ng GGC overnight. Cells were then cultured with the 1.2 Vα14 *i*NKT hybridoma overnight and IL-2 in the supernatant was quantified by ELISA. Data are representative of two independent experiments. Error bars represent ± SEM of three wells per condition. (B) Ex vivo antigen presentation assay. Mice with the WT CD1d gene replaced with a tail-deleted CD1d (TD) gene were injected i.v. with 1 μg of the indicated lipid Ags and at 22 h, splenic $CD11c^+$ DCs were enriched by magnetic bead isolation and varying numbers were co-cultured with 1.2 Vα14 *i*NKT hybridoma cells. Data are plotted as the number of enriched DCs per well versus IL-2 (U/mL) and are representative of mouse triplicates for each group for one of two independent experiments. Error bars represent ± SEM.

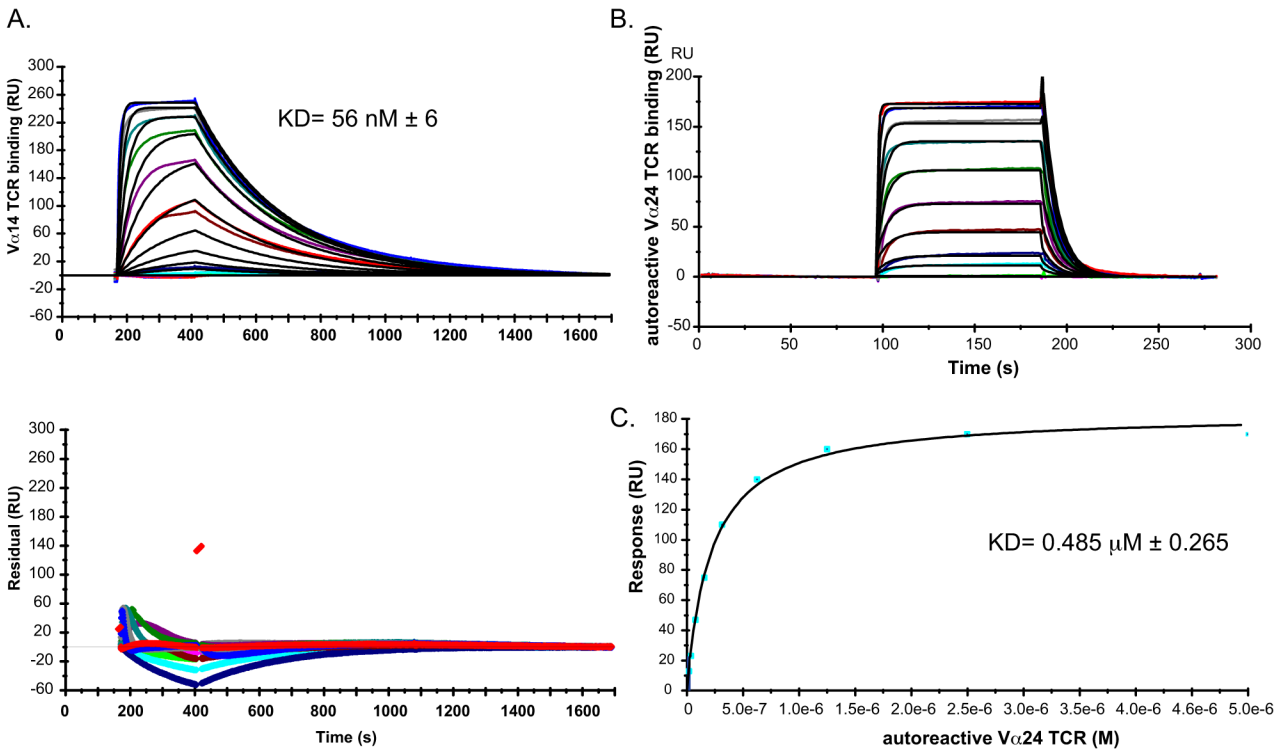

FIGURE 6. TCR binding to CD1d-DB06-1 complexes

(A) Biacore SPR sensorgram showing the binding of increasing concentrations of a mouse Vα14-Vβ8.2 *i*NKT cell TCR (0.004 to 2 μM) to complexes of mouse CD1d-DB06-1. Data are representative of three independent experiments. Bottom: Plot of the residuals, which is the deviation in the actual data from the fitted model. (B) Binding of an autoreactive human Vα24 *i*NKT cell TCR (0.2 to 5 μM) to human CD1d-DB06-1 complexes as assessed by SPR. Data are representative of three independent experiments. (C) Saturation plot demonstrating equilibrium binding of the human *i*NKT cell TCR to immobilized CD1d-DB06-1.

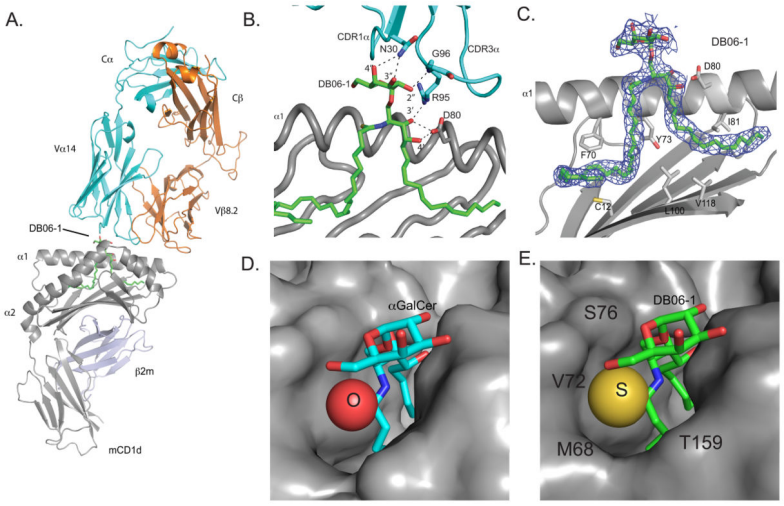

FIGURE 7. Crystal structure of the mouse CD1d-DB06-1-Vα14Vβ8.2 TCR ternary complex

(A) Overview of the ternary complex. PDB ID 4ZAK. (B) TCR/glycolipid Ag contacts. C.) Final $2F_0–F_c$ electron density map as shown as blue mesh, contoured at 1.0 σ level for the DB06-1 glycolipid. Note that the α2-helix is removed for clarity. (D, E) CD1d surface showing fit of αGalCer with oxygen highlighted (D) and DB06-1 with the sulfur and local amino acids highlighted (E).

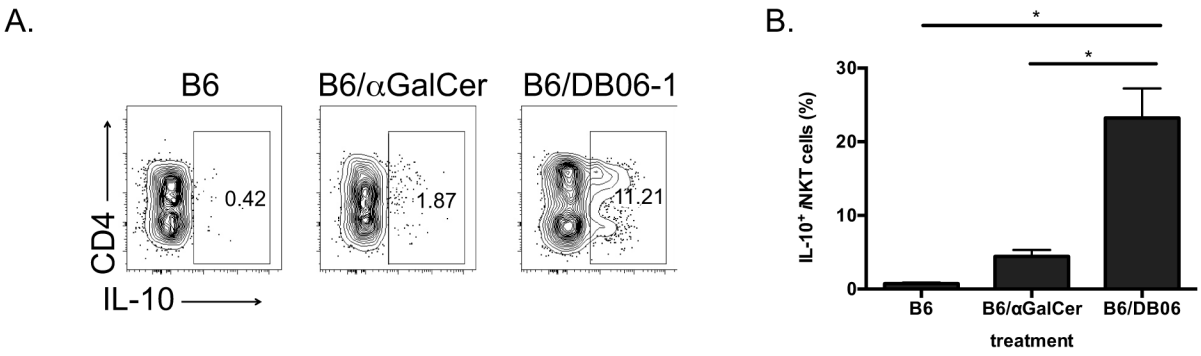

FIGURE 8. Increased IL-10 induced by DB06-1

(A, B) IL-10 production as measured by intracellular staining of splenic *i*NKT cells from C57BL/6 mice. *i*NKT cells were gated as live cells that were $B220^{-}$, $CD8\alpha^{-}$, $CD3\varepsilon^{+}$ and CD1d-tet^{+}. Mice were injected with 4 μg of the indicated Ags, DB06-1 or αGalCer one month prior. Cells were re-stimulated with PMA and ionomycin *in vitro* and intracellular IL-10 produced by $CD4^{+}$ and DN *i*NKT cells is shown. (A) Representative flow cytometry plots showing IL-10 production and (B) summary graph. Data are representative of two independent experiments. Error bars represent ± SEM of at least three mice per condition.